On POD Estimations with Radiographic Simulator aRTist

Christian GOLLWITZER[*], Carsten BELLON[*], Andreas DERESCH[*], Uwe EWERT[*],
Gerd-Ruediger JAENISCH[*]
[*]BAM Federal Institute for Materials Research and Testing,
Unter den Eichen 87, 12205 Berlin, Germany

Abstract. The computer simulation of radiography is applicable for different purposes in NDT such as for the qualification of NDT systems, the optimization of system parameters, feasibility analysis, model-based data interpretation, education and training of NDT/NDE personnel, and others. Within the framework of the European project PICASSO simulators will be adapted to support reliability assessments of NDT tasks. The radiographic simulator aRTist developed by BAM is well suited for this task. It combines analytical modelling of the RT inspection process with the CAD-orientated object description applicable to various industrial sectors such as power generation, aerospace, railways and others. The analytic model includes the description of the radiation source, the interaction of radiation with the material of the part, and the detection process with special focus to DIR. To support reliability estimations the simulation tool is completed by a tool for probability of detection (POD) estimation. It consists of a user interface for planning automatic simulation runs with varying parameters, specifically defect variations. Further, an automatic image analysis procedure is included to evaluate the defect visibility and calculate the POD therefrom.

Introduction

A general problem with NDT methods is the physical limitation of the applied measuring principle. Especially when a certain method is pushed to the limit, it constitutes a dangerous error to designate a part as "defect-free" when no defect has been found by the NDT method. Typically, flaws below some critical size are detected only with a certain probability <100% by a given method, and when the flaw size is further reduced, this probability quickly decreases such that it is highly unlikely to detect the flaw using the given method. Here, NDT reliability analysis comes into play which statistically estimates this probability of detection (POD) of a flaw given a characteristic parameter like its size or orientation. The method of determining the POD as a function of flaw size has been put forward by Alan Berens in his seminal work[1], and today it is well established in many industrial sectors like aeronautics, railway or power generation, requiring high standards for the respective NDT systems.

Despite its widespread use, the application of the POD determination following Berens is still quite costly, since the user has to manufacture a series of artificial defects with certain properties and analyze them using the NDT method in question. With the availability of NDT simulation systems achieving a high level of realism, it is tempting to replace the expensive inspection of artificially created test samples by cheap computer simulations, which can generate test data for large collections of defects much easier and faster. While there will be no way around testing the physical NDT system at least for

settings with high reliability requirements, it should be possible to combine simulated and experimental data to get NDT performance estimates faster and with reduced costs, or for estimating the NDT performance and determining requirements for systems that are not yet physically built. This is the aim of the European PICASSO project[2]. In the framework of PICASSO, the existing radiographic simulator aRTist[3] has been enhanced by a software module, SimuPOD, which facilitates the simulation of POD trials from within aRTist. It provides a user friendly interface to setup, perform, and analyze series of calculations with a special focus on POD curve estimation. In the following section, the POD method is shortly reviewed. Then we describe the aRTist software package and its improvements since the publication of Ref[3]. Finally, SimuPOD is described.

1. The POD(a) method

To estimate the POD as a function of the flaw size a, a series of defects must be manufactured with different a and measured using the NDT system in question. In the $\hat{a}$-vs-a analysis proposed by Berens[1], the NDT system is modelled by a two-stage process: first, a physical measurement produces the signal response $\hat{a}$ that is a strictly increasing function of the real size a, and this signal is further disturbed by noise. Then, a decision takes place whether $\hat{a}$ is larger than a given threshold $\hat{a}_{\mathrm{dec}}$, in which case, the NDT system signals the detection of a flaw. Under these circumstances the POD is given by the probability, that the measured $\hat{a}$ (including the noise) exceeds the threshold $\hat{a}_{\mathrm{dec}}$ [1]

$$(1) \qquad \mathrm{POD}(a) = \mathrm{P}\,(\hat{a} > \hat{a}_{\mathrm{dec}}).$$

The exact unit and meaning of $\hat{a}$ depend on the method. For example, in UT, $\hat{a}$ could mean the echo height of an indication, and in RT it can be the contrast. Berens postulates, that the functional relation of $\hat{a}$-vs-a can often be described by a linear function on a log-log scale, provided that the noise floor at small values of $\hat{a}<\hat{a}_{\mathrm{th}}$ and the saturation at large values of $\hat{a}>\hat{a}_{\mathrm{sat}}$ are removed from the data. He further proposes the use of censored linear regression to estimate this dependency from the measured data. For Gaussian white noise, the POD(a) curve is nothing but a properly scaled error function of **log** a, such that POD(a_{dec})=50%, where a_{dec} is the flaw size corresponding to the decision threshold $\hat{a}_{\mathrm{dec}}$. Since the POD curve determined by this method is itself a measured quantity, it is subject to statistical errors. Berens uses the method of Cheng&Iles[4] to infer a lower 95% confidence bound from the experimentally determined POD curve. The value $a_{90/95}$, where the POD of a flaw equals 90% within the 95% confidence band, is now generally accepted as the limit of an NDT system.

Using the framework described above, the following ingredients are necessary to estimate the POD: first, the parameters a and $\hat{a}$ must be defined for the given method. Second, a series of setups with trial defects must be prepared. Finally, the thresholds $\hat{a}_{\mathrm{dec}}$, $\hat{a}_{\mathrm{th}}$ and $\hat{a}_{\mathrm{sat}}$ must be set. All these settings can be controlled in a computer simulation; therefore it is possible to perform the whole process in a virtual setting.

In the next section, we give an overview of the radiographic simulation software package aRTist.

2. aRTist

The analytical RT inspection & simulation tool aRTist[3] is a software package for the simulation of X-ray imaging in industrial settings. It provides an interactive and user friendly 3D GUI to setup all parameters necessary for the simulation. Owing to the employed algorithm for image generation, it is also quite fast and achieves near interactive frame rates in typical settings.

The computation of an image in aRTist is a three-stage process. A first simulation computes the spectrum of the X-ray tube from the radiographic parameters. Alternatively, a measured spectrum can be loaded. The second stage casts rays from the source to every detector pixel and results in the dose value and the filtered spectrum for every pixel. The final stage converts the dose to gray values and applies noise characteristics and unsharpness. The computational engines for all three stages have undergone major revisiting in the newest version of aRTist. In the next sections, these modules are briefly described.

2.1 The source model

A quantitative model for the computation of realistic tube spectra, XRayTools[5], has previously been developed and is now integrated into aRTist. The model makes use of a built-in empirical function to estimate the electron density distribution in the target as a function of depth, direction and energy. Optionally, this distribution can be computed via Monte-Carlo simulations. The target is then subdivided into slices, and the radiation emission is summed over all slices. This summation takes into account Bremsstrahlung, primary and secondary characteristic radiation, and the attenuation of radiation emanating from deeper slices.
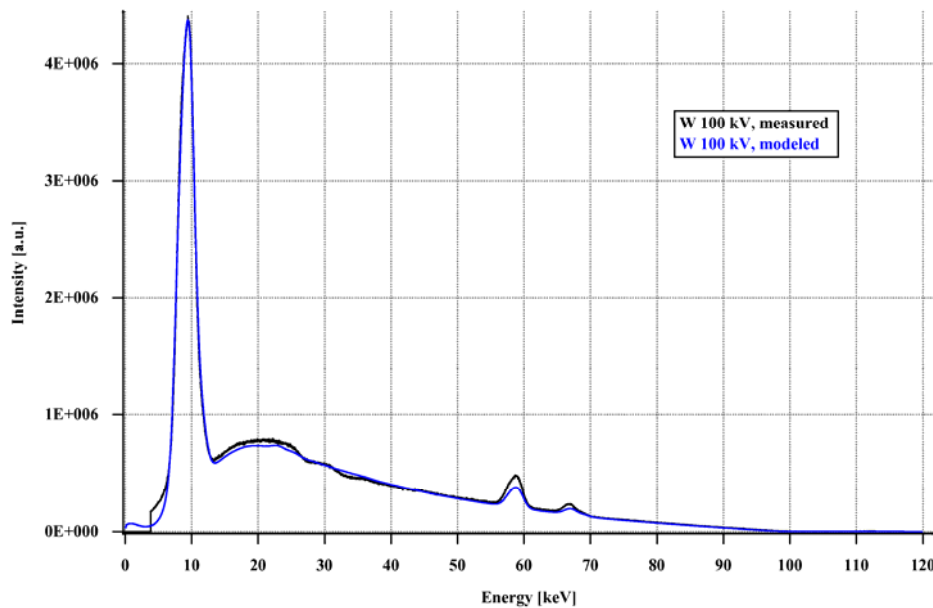

Figure 1. Spectrum of an X-ray tube with a tungsten target, acceleration voltage 100kV, target angle 24° and a 1mm beryllium exit window. Additional absorbers between the source and the detector are also taken into account.

Figure 1 displays a tube spectrum for 100kV acceleration voltage on a tungsten target. The black line represents a measurement with an AmpTek XR-100T-CdTe-stack detector, while the blue line is the result of the simulation of the whole experimental setting. All relevant features including the characteristic radiation are captured by the simulation. Note that the model has no adjustable parameters; especially the total radiation intensity is also predicted to good accuracy from the simulation. The deviation of the total photon flux in this example amounts to only 2.4%. The interested reader is referred to Ref[5] for further details.

2.2 The ray casting engine

In the second stage of the image generation, the intensity and spectrum of the radiation at every detector pixel is calculated by attenuating the input spectrum along each ray from the source point to the corresponding pixel. The input for this algorithm is a triangulated surface model of the test piece in the industry standard STL format. This way it is possible to work with arbitrary geometry and to interface directly with CAD software. The module first computes thickness maps which indicate the attenuating length for every material at the given detector pixel. Then, the spectrum is attenuated according to the Beer-Lambert law and the total dose is computed, possibly respecting the spectral sensitivity of the applied detector and the angle of incidence (see section 2.3).

The careful reimplementation of this stage has brought a significant performance boost, thanks to two techniques. First, the calculation of the attenuating lengths is parallelized using OpenMP, thus taking advantage of the now ubiquitous multi-core CPUs that are found even in standard office PCs. Second, the Beer-Lambert attenuation and the summation of the contributions of each energy bin is offloaded to the GPU via OpenGL shading language (GLSL). The resulting shader program runs much faster than the CPU even on typical onboard graphics processors. A benchmark scene with 2000×2000 pixels, 48000 triangles and 116 energy bins runs in 2.2s on a stock office PC with a 2.66GHz Intel Core2Quad CPU using 4 cores and an Intel onboard graphics chip. This is almost 25 times faster than the previous version of aRTist on the same machine, which needs 54s for this setup. When the frame size is reduced to 1000×1000 pixels, the computation is finished within 0.65s, reaching interactive frame rates.

2.3 The detector model

The last stage of the image generation converts the incoming radiation intensity to the output units of the selected detector. For digital detectors (IP and DDA) this comprises the application of the spectral sensitivity in the second stage, the conversion from the absorbed dose to gray values and the application of detector noise and unsharpness.
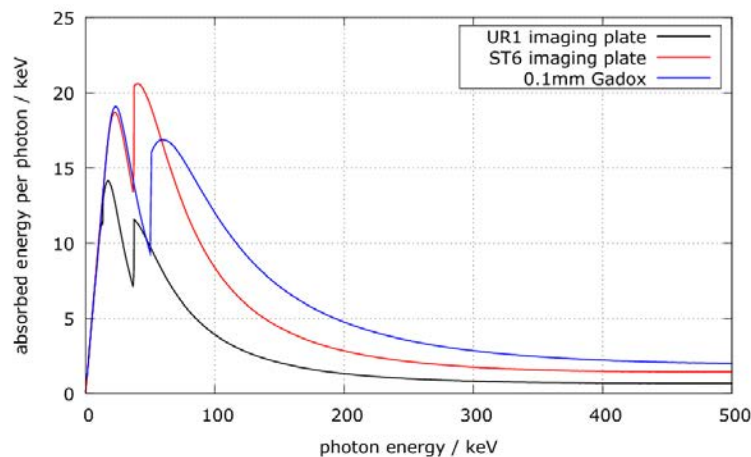

Figure 2. The spectral sensitivity of two different imaging plates and a typical scintillating screen for digital detector arrays as predicted by the detector model.

The spectral sensitivity of a given detector is modelled by the assumption, that the contribution of a photon to the final gray value is proportional to the mean deposited energy of the interaction of the photon with the sensitive layer of the detector. In the case of digital detectors, the sensitive layer is the scintillating screen, whereas for imaging plates it is the phosphor layer. This mean deposited energy per photon depends on the energy of the

photon and on the angle of incidence and in fact constitutes an upper bound on the sensitivity.

Figure 2 displays the spectral sensitivity predicted by the model for two different imaging plates and a typical scintillating screen as used for digital detector arrays. Preliminary experiments have been performed to verify this model, and they are found to be consistent with the predictions. A detailed comparison will be published in an upcoming article.

The conversion from the absorbed energy per pixel to a gray value contains many unknowns like amplifier settings, analogue integrator components and digital gain settings. Therefore, empirically determined conversion functions are employed to map the absorbed energy to an ideal gray value for every pixel. Next, noise is added with a noise power that matches the experimentally found signal-to-noise ratio dependent on the gray value. Finally, the image is convolved with an unsharpness kernel to match the spatial resolution of the real detector.

The output of the whole process is a simulated radiograph which closely matches experimental images. The consequent use of quantitative models results in realistic images and matching exposure times. The simulation of POD studies, detailed in the next section, relies on the quality of aRTist's engine as a basis.

3. SimuPOD

In order to simulate a POD study, it is necessary to set up a series of similar scenes, where the flaw geometry varies. To relieve the burden on the user of the simulation software, a good interface is needed which allows to define geometry variations without specifying individual parameters for each image, and to launch a batch run of the simulation. This is where SimuPOD comes into play. SimuPOD is an extension to aRTist with a user friendly GUI for defining series of calculations and running automatic analysis, with a special focus on POD studies. In the next sections, we describe the basic principles of SimuPOD's use and operation.

3.1 Defining series of defects

The interface of SimuPOD is built around the concept of *simultaneous variation of parameters,* which proves to be an efficient and easily understandable way to input many different scenarios of parameter variations. The GUI displays a set of parameters for each selected CAD part in the aRTist scene. These parameters refer to geometrical transformations of the objects in the 3D setting. CAD parts representing either test pieces or defects can be translated, scaled and rotated relative to their original position, and the X-ray source and the detector can also be translated. All these transformations happen in parallel. This can be thought of as a complex movement of the objects in question, thus the variation of the parameters for these transformations is dependent on time. The time is represented by the number of the current image. At each time step, the parameters of the transformations are computed for the current time, the objects are transformed, and images are generated. The exact formula which determines the movement is termed *distribution* and can be selected for every variable from a variety of presets or entered as a mathematical formula. Both deterministic as well as random variations are possible. With this concept, arbitrarily complex paths can be represented.
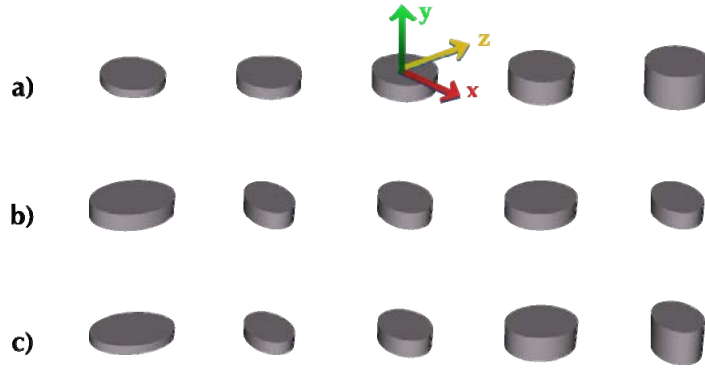
Figure 3. Variations of a cylindrical defect. a) logarithmically spaced increase in *y*-direction b) lognormally distributed size change in *z*-direction c) overlay of both variations.

As an example, consider a cylindrical defect with its axis of symmetry aligned to the world *y*-axis (Figure 3a). The length of the cylinder should later on serve as the primary size *a* in the *â*-vs-*a* analysis. When the scale factor in *y*-direction, *sy*, is set to vary logarithmically from 0.5 to 2, the length of the cylinder changes with a geometric progression from half of the original length to double the original length from the first to the last time step. Additionally setting the scale factor in *z*-direction, *sz*, to follow a lognormal distribution, leads to random geometric fluctuations of the cylinder perpendicular to its axis (Figure 3b,c). The fluctuations model the uncertainty of the flaw geometry of a real trial series where a single size parameter *a* is not sufficient to describe the entire geometric variation. This idea of introducing random variations into the computer simulation was developed by PICASSO[2] in the framework of the Monte Carlo POD method. Therefore, with only a few settings, an arbitrary large number of defect geometries with given size distributions can be generated.

When the simulation is started, SimuPOD computes three images for each time step: The radiograph including the defects, an additional radiograph without the defects, and the thickness map for the defects only. These image sets are needed for the automatic image analysis, which estimates the visibility of the defects in the images.

3.2 Automatic image evaluation

After the simulation is finished, the signal response *â* must be determined from the images. For this, SimuPOD includes a simple image analysis module which runs a model observer on the generated images. The model is a simplified ideal observer[6], which builds a linear combination of the defect free radiograph and the pure defect image to match the radiograph of the defective object. Then, the statistical significance of the defect image is evaluated. An in-depth discussion of this model observer will be published in a follow-up article.

The output of the model is a dimensionless number, which rates the visibility of the defect in every image. This is used as the signal response *â* in the POD(*a*) analysis. Figure 4a displays the result of a sample run, where the defect is a cylinder with its axis aligned parallel to the radiation direction. 70 samples have been drawn, where the length is varied with a logarithmic distribution over more than two decades, and the size in one perpendicular direction is varied randomly following a lognormal distribution with $\sigma=0.3$. The main source of the scatter is the artificially introduced geometry variation perpendicular to the axis. A second, much weaker source of noise is the simulated noise level of the radiographs.
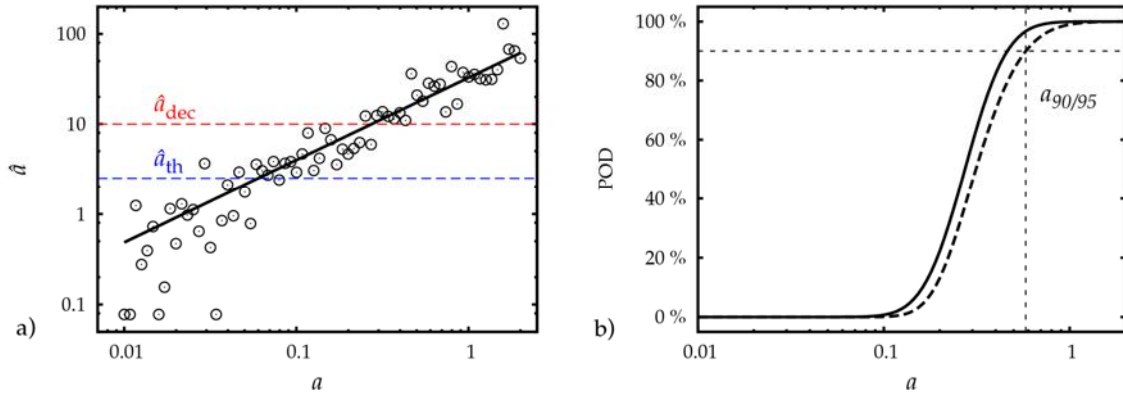
Figure 4. Result of the automatic image analysis of the defect variation in figure 3. a) $\hat{a}$-vs-a plot. The blue and red dashed lines represent the decision threshold $\hat{a}_{dec}=10$ and the signal threshold $\hat{a}_{th}=2.5$, respectively. b) POD curve corresponding to the data and thresholds in a) The dashed lines mark the flaw size $a_{90/95}$, where the 95% confidence bound crosses the 90% line.

3.3 Interactive POD estimation

After the determination of a and $\hat{a}$, the analysis proposed in Ref[1] is carried out. Here, SimuPOD supports the user by an interactive GUI to set the thresholds $\hat{a}_{dec}$, $\hat{a}_{th}$ and $\hat{a}_{sat}$ and to compute the POD. The $\hat{a}$-vs-a plot as in Figure 4a is shown on the screen, and the horizontal dashed lines representing the thresholds can be dragged with the mouse. The resulting POD (as in Figure 4b) is displayed below the $\hat{a}$-vs-a plot and updated in real time. Therefore, the operator gets a direct feedback of the influence of the threshold settings. Additionally, a mouse click on any data point in the $\hat{a}$-vs-a diagram opens the corresponding image in aRTist. Visually comparing the images side-by-side with the dataset is a useful tool to find reasonable decision thresholds. Eventually, the POD curve can be exported to ASCII format for further analysis by the user.

Conclusion

The radiographic simulator aRTist has been enhanced by the module SimuPOD, which facilitates the simulation of the classical experimental POD(a) analysis. A small number of user defined parameters is sufficient to configure a comprehensive series of defects for batch calculation. The defect visibility is automatically extracted from the simulated radiographs, and the resulting POD(a) is displayed. The parameters for the computation can be set in an interactive fashion by the user. Improvements to the source and detector model of aRTist's computational engine have led to more realistic images and a performance boost of a factor of up to 25. In the future, more sophisticated planning strategies, image and statistical analysis algorithms will be evaluated. aRTist, together with SimuPOD, provides a prototype platform for rapidly implementing these algorithms.

References

[1] Berens A.P., NDE reliability data analysis, *ASM Handbook* **17**, 689-701 (1989)

[2] The PICASSO project, http://www.picasso-ndt.eu/

[3] Bellon C., Jaenisch G.-R., aRTist - Analytical RT Inspection Simulation Tool, *Proceedings of the DIR2007*, http://www.ndt.net/article/dir2007/papers/s1.pdf

[4] Cheng, R.C.H. & Iles, T.C. One-sided confidence bands for cumulative distribution functions. *Technometrics* **30**, 155–159 (1988).

[5] Deresch A., Jaenisch G.-R., Bellon, C. & Warrikhoff, A. Simulation and experimental verification of X-ray spectra. *AIP Conf. Proc.* **1211**, 535-540 (2010).

[6] Gallas B.D., Barrett H.H. Validating the use of channels to estimate the ideal linear observer. *J. Opt. Soc. Am. A.* **20**,1725-1738 (2003)